



ISSN: 0975-833X

Available online at <http://www.journalcra.com>

International Journal of Current Research
Vol. 9, Issue, 03, pp.47343-47348, March, 2017

INTERNATIONAL JOURNAL
OF CURRENT RESEARCH

RESEARCH ARTICLE

SYNTHESIS OF PEROVSKITE MANGANITE $\text{La}_{1.25}\text{Sr}_{1.75}\text{Mn}_2\text{O}_7$ BY Sol Gel TECHNIQUE

*Tahereh Nekoukhou, Ana Khajehnejad and Seid Ali Sebt

Islamic Azad University, Science and Research Branch-Department of plasma

ARTICLE INFO

Article History:

Received 15th December, 2016

Received in revised form

09th January, 2017

Accepted 05th February, 2017

Published online 31st March, 2017

Key words:

Sol gel, Perovskite manganite,
Calcination, VSM.

Copyright©2017, Tahereh Nekoukhou et al. This is an open access article distributed under the Creative Commons Attribution License, which permits unrestricted use, distribution, and reproduction in any medium, provided the original work is properly cited.

Citation: Tahereh Nekoukhou, Ana Khajehnejad and Seid Ali Sebt, 2017. "Synthesis of Perovskite manganite $\text{La}_{1.25}\text{Sr}_{1.75}\text{Mn}_2\text{O}_7$ BY Sol Gel technique", *International Journal of Current Research*, 9(03), 47343-47348.

ABSTRACT

Perovskite manganite $\text{La}_{1.25}\text{Sr}_{1.75}\text{Mn}_2\text{O}_7$ (LSMO) were synthesized successfully by the sol gel technique. LSMO was synthesized at pH of 5 and at two calcination temperatures of 1250 and 1450 °C for 12 hours. Phase formation, structure and magnetic properties of LSMO was investigated by X-ray diffraction, scanning electron microscopy (SEM), EDS, FTIR and VSM. It was found that the calcination temperature influences on the size of crystallite and magnetic properties.

INTRODUCTION

Nanoscale manipulation of functional materials is generating a very broad interest in many fields such as electronics, optics, magnetism, ferroelectricity, or superconductivity because of its capability of improving the fundamental properties or even to generate dramatically new functionalities. Nano magnetism has become a very rich arena where new phenomena are being discovered with many potential applications in magnetic recording, spintronic, sensors, biomedicine and so on (Ross, 2001; Zheng and Wang, 2004). In addition, it has been shown that vortex pinning centers can be generated in superconducting films grown on top of surface nanotemplates (Foltyn and Civale, 2007), similarly to nanocomposite films (Gutierrez et al., 2007). Two general approaches, lithography and self-assembly, have been already found to be extremely successful in metallic and semiconducting nanostructure generation in surfaces (Barth et al., 2005; Shchukin and Bimberg, 1999; Teichert, 2002; Zheng and Wang, 2004). Complex oxides, instead, have only recently become an object of interest study. The formation of self assembled oxide nanostructures by vapor deposition techniques have been found to follow either the Volmer-Weber or Stranski-Krastanov mechanisms, similarly to semiconductor systems (Teichert, 2002), while chemical solution deposition (CSD) has been only started to be used as a powerful bottom-up nanofabrication methodology (Gibert et al., 2007; Gilbert, 2007). Three-dimensional self-organized nanocomposite films

have also very recently appeared as promising candidates for the generation of new physical phenomena, such as multiferroic behavior (Zheng et al., 2006), but also to tune their physical properties, such as magnetoresistance in a percolative transport system (Mosshnyaga et al., 2003). Among the complex oxides, rare earth manganites of the type $\text{Ln}_{1-x}\text{A}_x\text{MnO}_3$ (Ln is a rare earth, A is an alkaline earth) have become an extremely rich family of compounds displaying a wide variety of behavior, such as ferromagnetism, metallic conductivity, antiferromagnetism, colossal magnetoresistance, charge order, phase separation, insulating states, and so on (Coey et al., 1999; Salamo and Jaime, 2001; Tokura, 2006). Additionally, a strong link between these states can be induced, either by modified composition, oxygen stoichiometry or strain state, or by several types of external parameters, such as temperature, pressure, magnetic, electric fields, X-ray irradiation and so on. The metallic ferromagnetic phase $\text{La}_{1-x}\text{Sr}_x\text{MnO}_3$ with $x=0.3 - 0.4$ has been found to be one of the most robust manganites and hence it is often selected as a model system to investigate nanoscale phenomena.

Experimental procedure

Chemical grade metal nitrates $\text{La}(\text{NO}_3)_3 \cdot 6\text{H}_2\text{O}$, $\text{Sr}(\text{NO}_3)_2 \cdot \text{H}_2\text{O}$ and $\text{Mn}(\text{NO}_3)_2 \cdot 4\text{H}_2\text{O}$ and citric acid as a complex agent, were used. The above compounds were dissolved separately in de-ionized water to form solution. Then, the solutions were combined in stoichiometry ratios under magnetic stirring. The pH was adjusted to 5 by addition of ammonia while the solution was heated to 75 °C. After 7 hours, a black gel was

*Corresponding author: Tahereh Nekoukhou, Islamic Azad University, Science and Research Branch-Department of plasma

formed. After complete dissolution, the gel was centrifuged at the speed of 3500 and the separated solid portion was selected. The separated solid portion was heated at 110 °C for 24 hours in oven. The obtained powder was calcinated at two different temperatures (1250 and 1450 °C) for 10 hours to achieve the crystalline LSMO. The phase and structure of the products were characterized by X-ray diffractometer with CuK_{α} radiation by X'pert HighScore Plus software. The quantitative analysis of XRD patterns were done by material analysis using diffraction (MAUD) software and rietveld method. The point analysis of EDS of samples were done to justify the lack of impurities and unwanted heavy elements. To determine the morphology and the grain sizes of samples, the SEM was done by KYKY-EM3200 model. FTIR was used to reconfirm the XRD results. The magnetic properties of the products were measured by vibrating sample magnetometer.

RESULTS AND DISCUSSION

Figure 1 is a plot of XRD and calculated spectrum of sample S1 and S4 by MAUD software. The results are contained the composition, the size of crystallites and network parameters. Two main products produced were $La_7Sr_3MnO_3$ and $La_5Sr_{1.5}MnO_4$ and some minor impurities which for calcination

temperature of 1450 °C was higher than that of temperature 1250 °C. product $La_7Sr_3MnO_3$ had a rhombohedral crystalline structure and product $La_5Sr_{1.5}MnO_4$ had a tetragonal crystalline structure. Table 1 is the extracted parameters from Figure 1 which presents the quantitative values of XRD algorithms of Samples S1 and S4. The results indicate that by changing calcination temperature at 10 hours, it influences on composition of $La_7Sr_3MnO_3$ and $La_5Sr_{1.5}MnO_4$ products produced. Calcination temperature also affected on crystallite sizes. A decrease in calcination temperature from 1450 °C for sample S1 to calcination temperature of 1250 °C for sample S4, the crystallite size was reduced from 88.5 to 37 for compound $La_7Sr_3MnO_3$ respectively, and for product $La_5Sr_{1.5}MnO_4$ the crystallite sizes were reduced from 157.1 for sample S1 to that of 50.2 for sample S4 respectively. Figures 2 and 3 is a plot of EDS for sample S1 and S4 respectively. The point analysis of EDS shows unwanted heavy elements in samples S1 and S2 in both calcination temperatures of 1450 and 1250 °C respectively. Figures 4 and 5 are SEM plot for samples S1 and S4 respectively. The results indicate that with increasing calcination temperature the size of crystallite decreases and less homogeneity was obtained. The morphology of grain are spherical at calcination temperature of 1450 °C for sample S1 in comparison to that of sample S4 at temperature 1250 °C

Table 1. The quantitative values of XRD algorithms for samples S1 and S4

Sr(NO ₃) ₂	MnO ₂	SrO	La ₂ O ₃	La ₅ Sr _{1.5} MnO ₄	La ₇ Sr ₃ MnO ₃	Phase
0.4wt%	8.6wt%	0.1wt%	3.1wt%	38.5wt%	58.3wt%	S1 composition
-	-	-	-	55.5wt%	34.3wt%	S4 composition
-	-	-	139±6.3	157.1±9	88.5±6.8	crystallite size(nm) for S1
231.9±21.9	99.7±18.8	115.1±21.4	-	50.2±2.1	37±4.7	crystallite size(nm) for S4
-	-	-	a=3.9 c=6.1	a=3.4 c=12.5	a=5.5 b=13.4	Network parameter for S1(A ⁰)
a=7.8	a=4.5 c=2.8	a=5	-	a=3.8 c=12.4	a=5.5 c=13.4	Network parameter for S4(A ⁰)

Table 2. Magnetic parameters obtained from Figure 8 for Samples S1 and S4

S4	S1	Sample
7.3	10.9	Magnetism (emu/g)

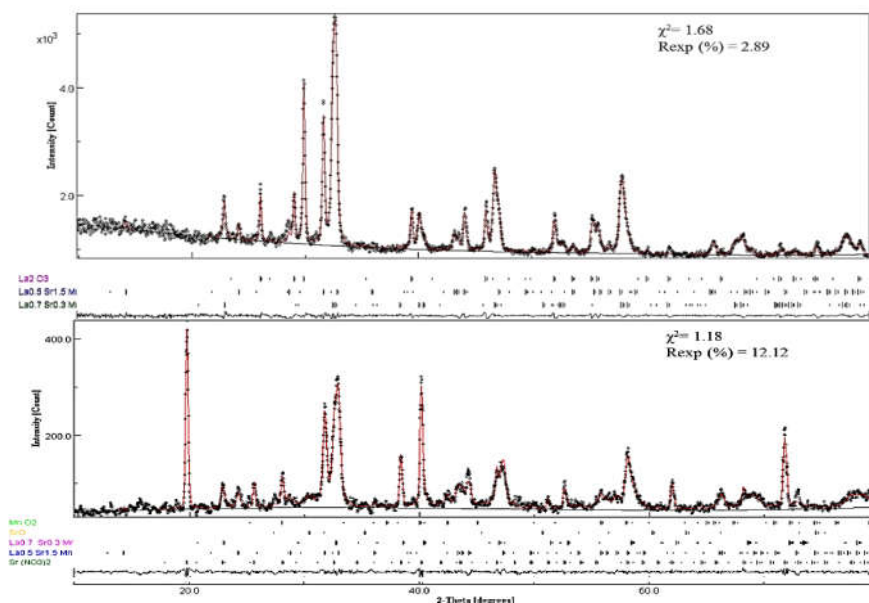


Fig.1- XRD pattern and calculated Spectrum by MAUD software for Samples S1 and S4.

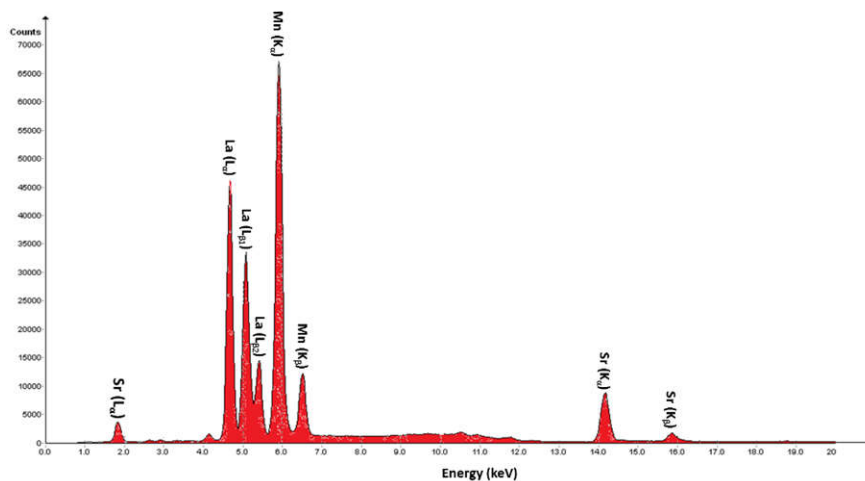


Fig.2- EDS of sample S1 prepared at PH=5, calcination temperature of 1450 °C for 10 hours.

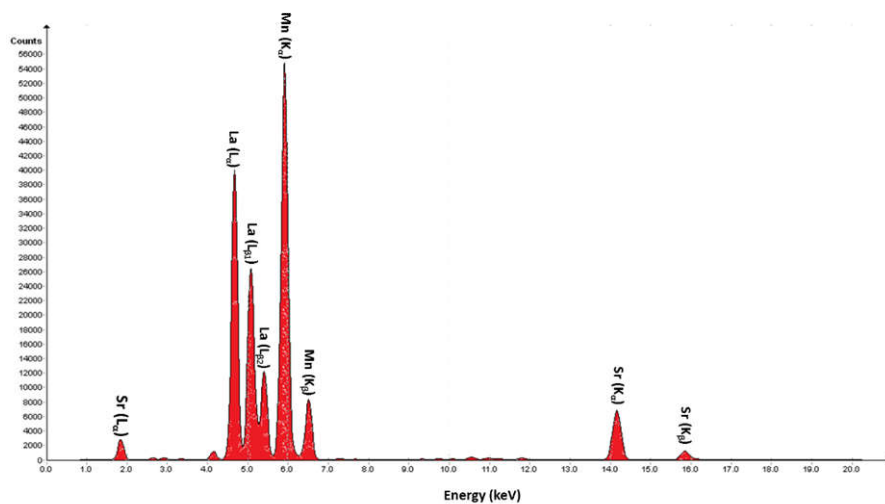


Fig.3- EDS of sample S4 prepared at PH=5, calcination temperature of 1250 °C for 10 hours.

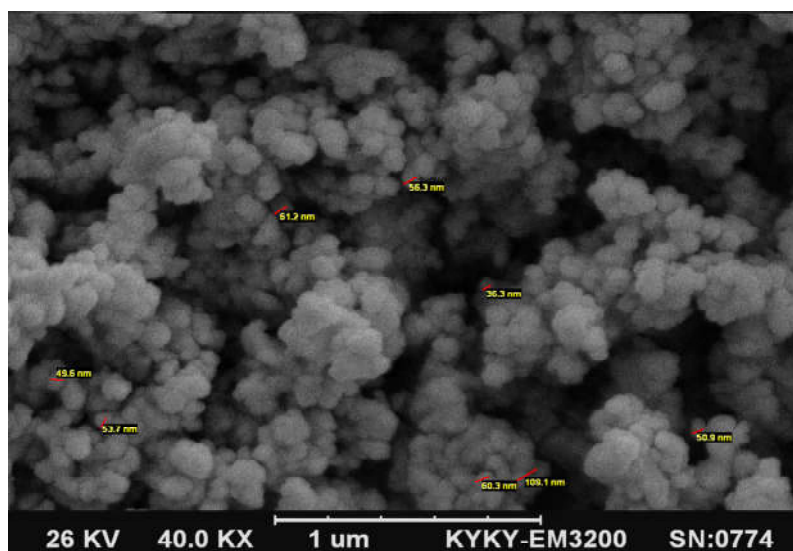


Fig.4- SEM of sample S1 prepared at pH=5, calcination temperature of 1450 °C for 10 hours.

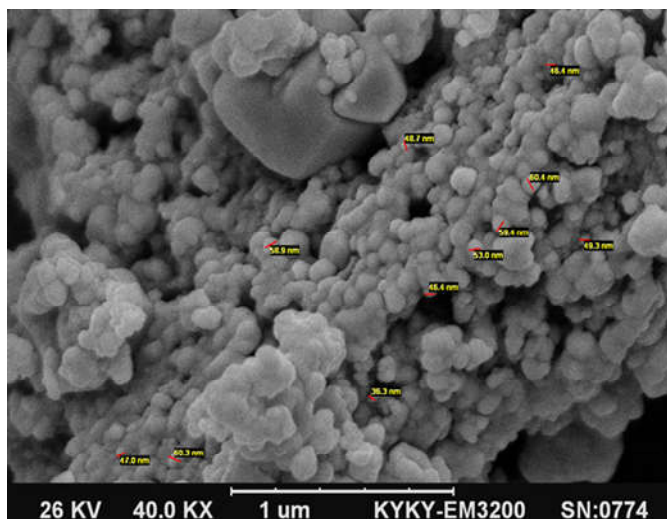


Fig.5- SEM of sample S4 prepared at pH=5, calcination temperature of 1250 °C for 10 hours.

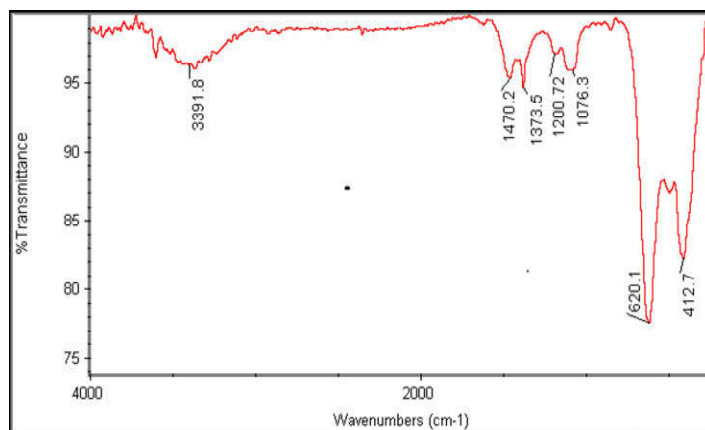


Fig.6-FTIR for sample S1 prepared at PH=5, calcination temperature of 1450 °C for 10 hours.

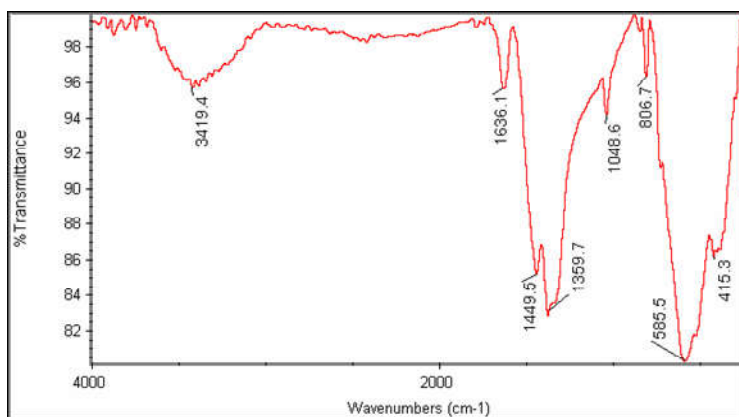


Fig.7-FTIR for sample S4 prepared at PH=5, calcination temperature of 1250 °C for 10 hours.

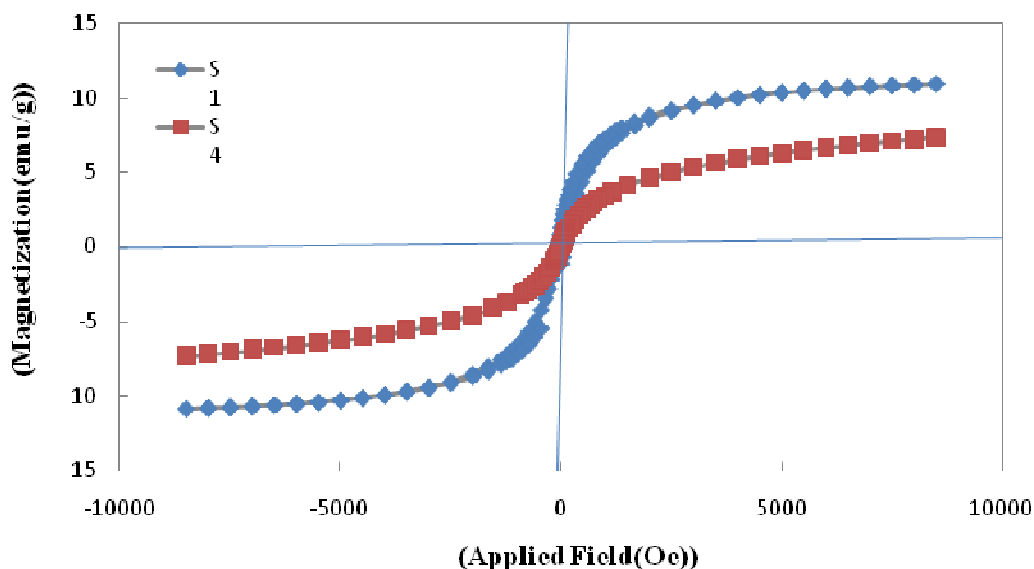


Fig.8. VSM hysteresis loops of samples S1 and S4

which some were agglomerated. Figures 7 and 8 are plots of FTIR for samples S1 and S4 respectively. The results in these figures show the absence of some hydrocarbon impurities and also a justification for formation of crystalline spaces containing metallic cations. Absorptive spectrum in range of 400 and 600 cm^{-1} is related to MnO_6 (Rostamnejadi *et al.*, 2009). This is an indicative for formation of perovskite structure of LSMO (Gupta *et al.*, 2012). Absorptive spectrum at range of 737, 815, 1387 and 1440 cm^{-1} are related to strontium nitride (Miller and Wilkins, 1952). Absorptive spectrum at range of 851 and 1455 cm^{-1} is related to strontium carbonate (Gupta *et al.*, 2012). Intense reduction in strontium nitrate peaks in S1 sample in comparison to that of sample S4 is another reason for noticeable reduction of this compound in Sample S1. Of course with regard to performance mechanism of FTIR and XRD, the absence of this phase in XRD algorithm for S1 sample is due to its non-crystalline properties of this compound.

Figure 8 is a plot of VSM hysteresis loops for sample S1 and S4. Magnetism in samples are function of composition, crystallite size, crystalline network parameter, cationic distribution and the degree of crystallinity. The results in Fig.8 shows ferromagnetism behavior for both samples (S1 and S4). The extracted saturated magnetic values from figure 8 for samples S1 and S4 are given in Table 2.

S1 sample with calcination temperature of 1450 $^{\circ}\text{C}$ for 10 hours showed higher magnetic behavior than that of sample S4 with calcination temperature of 1250 $^{\circ}\text{C}$ for 10 hours.

Conclusion

Based on the results obtained from this research the following conclusion can be drawn:

- 1- Nano particles of LSMO was produced successfully by So-gel techniques at PH=5, calcination temperatures of 1250 and 1450 $^{\circ}\text{C}$ for 10 hours.
- 2- XRD algorithm and FTIR both confirmed the formation of LSMO with perovskite structure and composition of $\text{La}_{0.7}\text{Sr}_{0.3}\text{MnO}_3$ and $\text{La}_{0.5}\text{Sr}_{0.5}\text{MnO}_4$.

- 3- With an increase in calcination temperature for 10 hours the crystallite size was increased.
- 4- The presence of suitable cations in compounds was confirmed by EDS analysis and the absence of heavy elements was proved.
- 5- Higher magnetic behavior was obtained for the sample with higher calcination temperature.

REFERENCES

- Barth, J.V., Costantini, G. and Kern, K. 2005. "Engineering atomic and molecular nanostructures at surfaces" *Nature*, 437(7059), PP. 671-679.
- Coey, J.M.D., Viret, M. and Von Molnar, S. 1999. "Mixed valence manganites" *Advances in Physics*, 48(2), PP.167-293.
- Foltyn, S.R., Civale, L., etc., 2007. "Materials science challenges for high-temperature superconducting wire" *Nat. Mater.*, 6(9), PP. 631-642.
- Gibert, M., Puig, T. and Obradors, X. 2007. "Growth of strain-induced self assembled BaZrO_3 nanodots from chemical solutions" *Surf. Sci.*, 601(13), PP. 2680-2683.
- Gilbert, M., Puig, T., Obradors, X., Benedetti, A., etc., 2007. "Self-organization of Heteroepitaxial CeO_2 NANODOTS Grown from chemical solution" *Adv. Mater.*, 19(22), PP.3937-3942.
- Gupta, M., P. Yadav, W. Khan, A. Azam, etc. 2012. "Low temperature synthesis and magneto resistance study of nano $\text{La}_{1-x}\text{Sr}_x\text{MnO}_3$ ($x=0.3, 0.33$ and 0.4) perovskites," *Adv. Mat. Lett.*, Vol.3, PP.220-225.
- Gutierrez, J., LLordes, A., Gazquez, J., etc., 2007. "strong isotropic flux pinning in solution-derived $\text{Y Ba}_2\text{Cu}_3\text{O}_{7-x}$ nanocomposite superconductor films" *Nat. Mater.*, 6(5), PP. 367-373.
- Miller F.A. and C.H. Wilkins, 1952. "Infrared spectra and characteristic frequencies of inorganic ions," *Analytical Chemistry*, Vol.24, PP. 1253-1294.
- Mosshnyaga, V., Damaschke, B., Shapoval O., etc. 2003. "Structural phase transition at the percolation threshold in epitaxial $(\text{La}_{0.7}\text{Ca}_{0.3}\text{MnO}_3)_{(1-x)} : (\text{MgO})_{(x)}$ nanocomposite films" *Nat. Mast.*, 2(4), PP. 247-252.

- Ross, C.A. 2001. "Patterned magnetic recording media" *Annu. Rev. Mater. Res.*, 31(1), PP.203-235.
- Rostamnejadi, A., H. Salamati, P. Kameli and H. Ahmadvand, 2009. "Superparamagnetic behavior of $La_{0.67}Sr_{0.33}MnO_3$ nanoparticles prepared via sol-gel method" *Journal of Magnetism and Magnetic Materials*, Vol. 321, PP.3126-3131.
- Salamon, M.B. and Jaime, M. 2001. "The physics of Manganites: Structure and transport" *Rev. Mod. Phys.*, 73(3), PP.583-628.
- Shchukin, V.A. and Bimberg, D. 1999. "Spontaneous ordering of nanostructures on crystal surfaces" *Reviews of Modern Physics*, 71(4), PP. 1125-1171.
- Teichert, C. 2002. "Self-organization of nanostructures in semiconductor heteroepitaxy," *Physics Reports-Review Section of Physics Letters*, 365(5-6), PP. 335-432.
- Tokura, Y. 2006. "Critical features of Colossal magnetoresistive manganites" *Reports on Progress in Physics*, 69(3), PP. 797-851.
- Zheng, H. M., Straub, F., Zhan, Q., Yang, P. L., etc. 2006. "Self-assembled growth of $BiFeO_3$ - $CoFe_2O_4$ nanostructures" *Adv. Mater.*, 18(20), PP. 2747-2752.
- Zheng, H., Wang, J., Etc., 2004. "Multiferroic $BaTiO_3$ - $CoFe_2O_4$ nanostructure" *Science*, 303(5658), PP.661-663.
